Supporting Information

Ultra-rapid and highly selective colorimetric detection of hydrochloric acid via an aggregation to dispersion change of gold nanoparticles

Kehui Zhang,[a] Mingyue Luo,[a] Honghong Rao,[b] Haile Liu,[a] Ruibin Qiang,[a] Xin Xue,[c] Jianying Li,[a] Xiaoquan Lu[a] and Zhonghua Xue[a]*

[a] Key Laboratory of Water Security and Water Environment Protection in Plateau Intersection (NWNU), Ministry of Education; Key Lab of Bioelectrochemistry and Environmental Analysis of Gansu Province, College of Chemistry and Chemical Engineering, Northwest Normal University, Lanzhou, 730070 (China)

[b] School of Chemical Engineering, Lanzhou City University, Lanzhou, 730070 (China)

[c] State Key Laboratory of Applied Organic Chemistry and Key Laboratory of Nonferrous Metal Chemistry and Resources Utilization of Gansu Province, Lanzhou University, Lanzhou, 730000 (China)

E-mail address: xzhlab@hotmail.com (Z. H. Xue).

Materials and regents

$HAuCl_4 \cdot 4H_2O$ was provided by Sigma-Aldrich. Reduced glutathione (GSH), trisodium citrate, 3,3′,5,5′-tetramethylbenzidine (TMB), hydrogen peroxide (H_2O_2), $FeCl_3$, $Cd(NO_3)_2$, $Pb(NO_3)_2$, $Hg(NO_3)_2$, hydrochloric acid (HCl), sulfuric acid (H_2SO_4), nitric acid (HNO_3), phosphoric acid (H_3PO_4), acetic acid (HAc), boric acid (H_3BO_3), oxalic acid, salicylic acid, NaCl, NaClO, hydrofluoric acid (HF), hydrobromic acid (HBr), and hydroiodic acid (HI) were purchased from Sinopharm Chemical Reagent. And the water used in all the experiments was obtained from Ulupure UPT-II system (18.24 MΩ·cm).

Instrumentation

UV-vis absorption spectra were measured by a T6 new century UV-vis spectrophotometer. Transmission electron microscopy (TEM) images were measured by an FEI Tecnai G2 F20 STwin. X-ray photoelectron spectroscopy (XPS) was obtained by an ESCALAB 250Xi (Thermo Fisher Scientific, USA). X-ray diffraction (XRD) was measured by an X-ray diffractometer (XRD-6000 Shimadzu). Fourier transform infrared (FTIR) spectra were measured by a Nicolet iS5 FTIR spectrometer (Thermo Fisher Scientific, USA). Dynamic light scattering (DLS) and Zeta potential data were recorded by a Zetasizer Nano ZS ZEN3600 system (Malvern Instruments, UK).

Synthesis of GSH-AuNPs.

The synthesis of GSH-AuNPs was referred to in the previously reported literature with slight modifications.[1] Specifically, 45 mL of ultrahigh purity water, 2.5 mL of $HAuCl_4 \cdot 4H_2O$ (5×10^{-3} M), and 2.5 mL of trisodium citrate (1.7×10^{-2} M) were added to a 100 mL round-bottom flask equipped with a condenser. Subsequently, the mixed solution was heated to reflux at 100˚C for 10 min. Then, the mixed solution was cooled naturally to room temperature, and was further injected with 300 μL of GSH (2.5×10^{-3} M) under magnetic stirring. After that, the mixed solution was stirred for 1 h. Finally,

the mixed solution was washed by centrifugation (6000 rpm, 10 min) at room temperature and dispersed in ultrapure water to obtain the wine-red GSH-AuNPs product.

Preparation of different GSH-AuNP aggregates.

According to previous literature, amino-binding effect-induced GSH-AuNP aggregates were obtained by adding Fe^{3+} and Cd^{2+} ions (10 μL, 10 mM) to 300 μL of GSH-AuNPs solution at pH 9.0.[2] Carboxy-binding effect-induced GSH-AuNP aggregates were obtained by adding Pb^{2+} ions (10 μL, 10 mM) to 300 μL of GSH-AuNPs solution at pH 8.0.[2] Electrostatic effect-induced GSH-AuNP aggregates were obtained by adding HNO_3 and HAc (10 μL, 20 mM) to 300 μL of GSH-AuNPs solution. In addition, centrifugal effect-induced GSH-AuNP aggregates were obtained by high-speed centrifugation (12000 rpm, 20 min).

Colorimetric detection of HCl in aqueous medium based on redispersion of GSH-AuNP aggregates.

The detection process used Pb^{2+} ions-induced GSH-AuNP aggregates as the sensing probes, in simple terms, 700 μL of different concentrations of HCl were directly added to 300 μL of Pb^{2+}-GSH-AuNP aggregates solution and the reaction was completed within 1 s. After the reaction system was stabilized, the digital camera and the UV-Vis spectrophotometer were used to record the color and the UV-Vis spectrum of the mixed solutions with different HCl concentrations, respectively.

Following the same procedure as above, various interferents (H_2SO_4, HNO_3, H_3PO_4, HAc, H_3BO_3, oxalic acid, salicylic acid, NaCl, NaClO, HF, HBr, HI) were chosen to verify the selectivity of HCl detection.

Colorimetric detection of HCl in the real sample.

To verify the practicality of the method, we chose tap water, Yellow River water, and lake water

as the actual samples. Among them, tap water need no further treatment, but Yellow River water and lake water were filtered twice through a 0.22 μm microfiltration membrane. In addition, we also learned that for the washing water in the chlorobenzene production process, it usually contains mainly HCl (8%-10%), Fe^{3+} (2000-8000 mg/L), and chlorobenzene (1000 mg/L). For this purpose, we prepared this industrial wastewater in the laboratory and diluted it 20 times (at this time, the concentration of HCl was 5000 ppm). Finally, all the above samples were tested by our proposed methodology.

Characterization of GSH-AuNPs

To demonstrate the successful preparation of GSH-AuNPs, we characterized their structure by UV-vis spectra, TEM, XRD, and XPS. As shown in Fig. S1A, the prepared GSH-AuNPs solution was wine-red in color and had a characteristic absorption peak at 530 nm. It could be observed from the TEM image that the GSH-AuNPs were well dispersed and had a size of about 20 nm or so (Fig. S1B). The lattice stripe spacing of 0.24 nm could be observed in the high-resolution transmission electron microscopy (HRTEM) image in Fig. S1B, which was caused by a group of (111) planes in the face-centered cubic (fcc) structure of Au^0.[3] Correspondingly, we also observed four characteristic crystalline peaks of GSH-AuNPs in XRD measurements (Fig. S1C), which originated from (111), (200), (220) and (311) plane diffraction of AuNPs, respectively, according to JCPDS 04-0784,[4] suggesting that our prepared GSH-AuNPs are well crystallized. In addition, the core-level Au 4f XPS profile of GSH-AuNPs (Fig. S1D) showed two characteristic XPS peaks at 84.2 eV (Au^0 $4f_{5/2}$) and 87.9 eV (Au^0 $4f_{7/2}$), suggesting that $HAuCl_4$ has been fully reduced to Au^0.[5] In summary, we demonstrated the successful preparation of GSH-AuNPs, which could be further used in the subsequent detection process.

Stability of aggregated GSH-AuNPs after redispersion.

To investigate the stability of the aggregated GSH-AuNPs after redispersion, we compared the color and SPR peak changes of the redispersed GSH-AuNP aggregates solution at 0.5, 1, 2, 3, 5, 10, 20, and 30 h. As shown in Fig. S5A, as time went on, the color of the solution gradually changed from wine-red to colorless, and the SPR peak kept damping until it disappeared completely (Fig. S5B), which might be the result of the dissolution effect of HCl on AuNPs, resulting in the change of GSH-AuNPs to gold chloride species ($[Au(Cl)_2]^-$ or $[Au(Cl)_4]^-$).[6] Using the commonly used ratio of absorbance at 630 nm to absorbance at 530 nm (A_{630}/A_{530}) to quantitatively evaluate the dissolution of AuNPs (Fig. S5C), it could be observed that the redispersed AuNPs were completely dissolved 10 h after the addition of HCl.

Optimization of HCl detection conditions

In order to make the method better for HCl detection in aqueous media, we first optimized some key conditions in the sensing process with A_{630}/A_{530}. It is worth noting that the detection method is very simple and only requires the addition of GSH-AuNP aggregates for the detection, so we only optimized the concentration of GSH-AuNPs. As shown in Fig. S6, with the increase of GSH-AuNPs concentration, A_{630}/A_{530} exhibited a trend of decreasing and then increasing, and reached the lowest point at the GSH-AuNPs concentration of 300 μL/mL, indicating that the aggregated GSH-AuNPs at this concentration had a better redispersion effect. Therefore, we used 300 μL/mL of GSH-AuNPs as the standard concentration for subsequent assays.

Selectivity study on HF, HBr, and HI

To further explore the effects of HF, HBr, and HI on the selectivity of the sensing methods, we selected different concentrations of HF, HBr, and HI to be added to the reaction system. After the reaction was stabilized, no obvious redispersion of GSH-AuNP aggregates was observed (Fig. S7),

indicating that the proposed sensing system has good selectivity for HCl. It is worth mentioning that HBr with 25000 ppm was added into the reaction system, the color of the solution changed to a faint dark-red rapidly, and then started to change to gray-blue after only 1-2 s and ultimately turned to gray-blue completely within 20 s (Fig. S8). As far as our proposed sensing method, HCl-triggered redispersion of aggregated GSH-AuNPs depends on two processes, i.e., protonation and hydrogen bond with surface GSH ligands. As well known, for HF, HCl, HBr, and HI, the order of acidic intensity is HI > HBr > HCl > HF, and the hydrogen bond intensity is F > Cl > Br > I.[7] Based on this, we believe that HF could not fully protonate GSH and therefore has no interference with HCl sensing in our observations. To verify this hypothesis, we measured the pH of the HF solution with 25000 ppm and found it to be only 2.5. However, for the HCl solution of 10000 ppm, it could already reach 1.5 (Note that the pH of 2.0 for this HCl solution obtained by a pH paper was provided in the manuscript, whereas the result here were obtained using a pH meter. Herein, we have modified it in the revised manuscript). According to the CAS database (70-18-8), the pKa values of GSH are pK1 = 2.12, pK2 = 3.53, pK3 = 8.66, and pK4 = 9.12 (at 25 ˚C), respectively. Therefore, although F could form the stronger hydrogen bond, but could not realize GSH protonation due to the lower pH of HF, thereby resulting in an inability to redisperse of GSH-AuNP aggregates.

As far as the interference of HBr and HI for HCl sensing, the main reason we believe that is the hydrogen bond formed by Br and I is not strong enough. It has been verified by HBr-related proved experiments shown in Fig.S8 in the Supporting Information. Where only less obvious dispersed observation of GSH-AuNP aggregates was obtained for a 2.5-fold higher concentration of HBr than HCl, and importantly the observed phenomenon then disappeared within 20 s. It may be attributed to the extremely unstable property of weaker hydrogen bond formed by Br in the system. Additionally,

we attempted to record this transitory phenomenon using the UV-Vis spectrophotometer, but failed due to the unstable reaction process. For the interference of HI, no any color change could be observed in the testing experiment, maybe due to the more weaker hydrogen bond compared to HBr.

The detection performance of the method for real samples

We designed the experiment initially to construct a rapid and simple POCT method for the detection of HCl in aqueous medium, and to use it for the detection of HCl-contaminated water to safeguard human health. For this reason, we collected tap water, Yellow River water and lake water samples and examined them by our method. As a result, no significant HCl contamination was found in these three real samples due to the lower content of HCl (<5 ppm). Therefore, we simulated the contaminated tap water, Yellow River water, and lake water by adding HCl (4000, 8000, and 10000 ppm) to these three samples, and found that the recoveries of the tap water, Yellow River water, and lake water were 92.2%-105.5%, 91.0%-104.0%, and 96.3%-103.1% (Table S3), respectively, indicating that the interferents therein do not affect the results of the assay when HCl contamination events occur in such environmental water samples.

In addition, we tested the formulated industrial wastewater directly with our proposed method and detected a concentration of 4997 ppm (Table S3), indicating that the interferents in this type of industrial wastewater do not affect the assay results significantly. Meanwhile, we further added 3000 and 5000 ppm of HCl for recovery assay, and the recoveries reached 90.7-95.9% (Table S3), which further proved that our proposed method has good reliability and practicability.

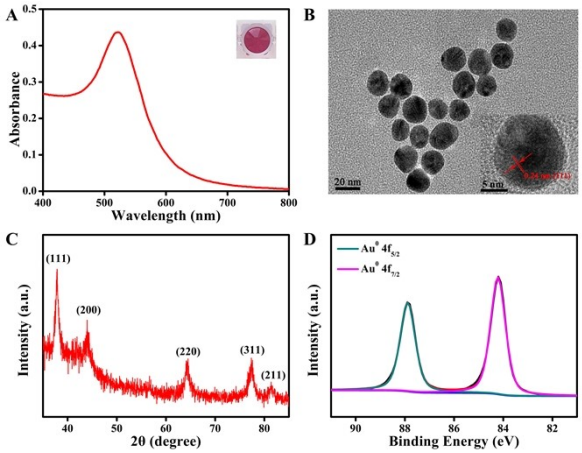

Fig. S1 (A) Solution color and Vis-NIR spectra of GSH-AuNPs. (B) TEM and HRTEM image of GSH-AuNPs. (C) XRD pattern of GSH-AuNPs. (D) The core-level Au XPS profile of GSH-AuNPs.

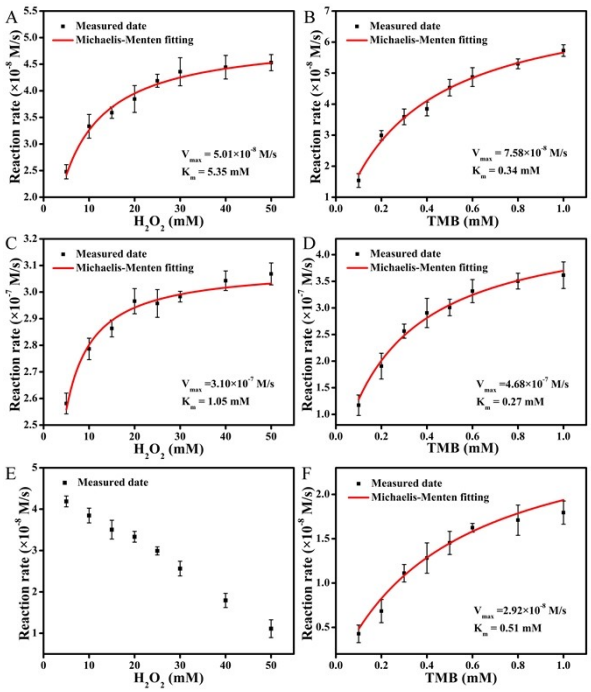

Fig. S2 Catalytic kinetic plots of GSH-AuNPs, GSH-AuNPs + Hg^{2+}, and GSH-AuNPs + Hg^{2+} + HCl for H_2O_2 (A, C, and E) and TMB (B, D, and F).

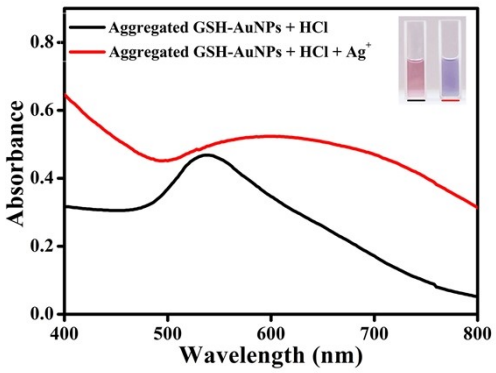

Fig. S3 Solution colors and Vis-NIR absorption spectra of Hg^{2+}-GSH-AuNP aggregates with HCl and Ag^{+} ions-treated HCl added, respectively.

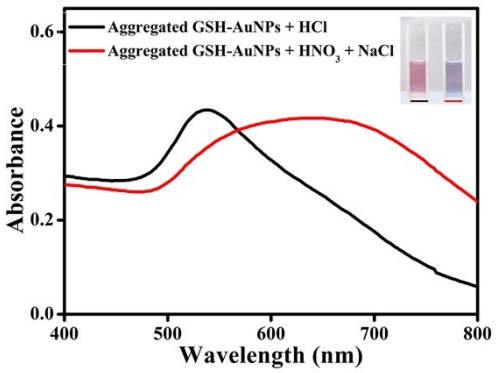

Fig. S4 Solution colors and Vis-NIR absorption spectra of Hg^{2+}-GSH-AuNP aggregates with HCl and HNO_3-NaCl added, respectively.

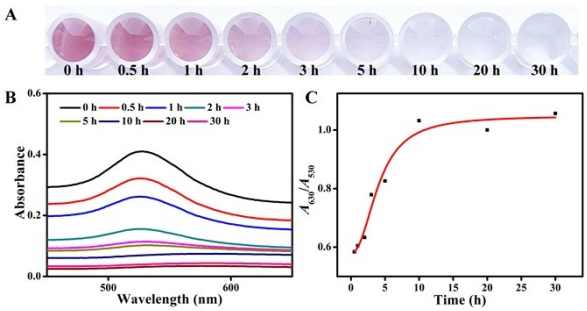

Fig. S5 Solution colors (A), Vis-NIR absorption spectras (B), and A_{630}/A_{530} values of the redispersed GSH-AuNP aggregates at 0.5, 1, 2, 3, 5, 10, 20, and 30 h.

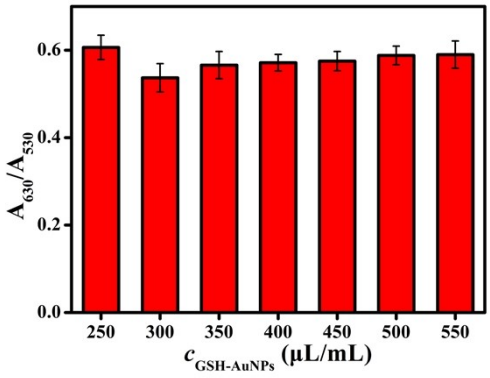

Fig. S6 Effects of GSH-AuNP aggregates concentration on the assay system for the detection of HCl.

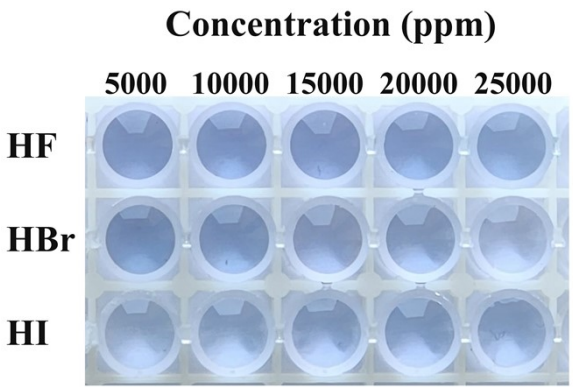

Fig. S7 Corresponding solution color changes produced when different concentrations of HF, HBr, and HI were added to the reaction system.

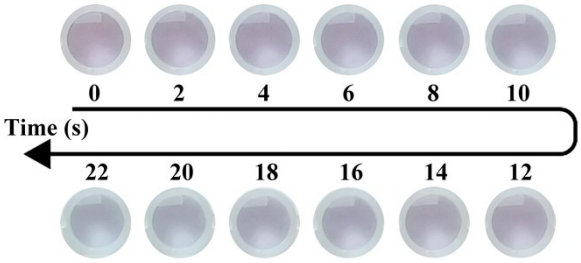

Fig. S8 Change of solution color with time after HBr is added to the reaction system.

Table S1. Comparison of the kinetic parameters of GSH-AuNPs, GSH-AuNPs + Hg^{2+}, and GSH-AuNPs + Hg^{2+} + HCl.

	Substrate	K_m (mM)	V_{max} (M/s)
GSH-AuNPs	TMB	0.34	7.58×10^{-8}
	H_2O_2	5.35	5.01×10^{-8}
GSH-AuNPs + Hg^{2+}	TMB	0.27	4.68×10^{-7}
	H_2O_2	1.05	3.10×10^{-7}
GSH-AuNPs + Hg^{2+} + HCl	TMB	0.51	2.92×10^{-8}
	H_2O_2	-	-

Table S2. Comparison of the sening performance of different HCl assays.

Methods	Sample	Material	Time	Linear Range	LOD	Selectivity	Ref.
Fluorescent	Gas	Nanofilm	10 min	0.15 ppm – 96 ppm	0.15 ppm	Air, H_2O, DCM, TCM, CCl_4, acetone, benzene, toluene, MeOH, EtOH, isopropanol, *n*-BuOH, *n*-pentane, *n*-hexane, *n*-heptane, DMF, DIPA, *o*-toluidine, aniline, NH_3, TEA, MA	[8]
Fluorescent	Gas	ZnMOF	5 s	-	2.63 ppm	HBr, HCl sol., HNO_3, NH_3	[9]
Colorimetric	Gas	Cu_4I_4-MOF	30 min	2.4 ppb – 3.2 ppb	2.4 ppb	HF, HBr, HI, HOAc, HNO_3, $HClO_4$	[10]
Resistance	Solution	Ppy	>1h	5 μM – 10 mM	5 nM	-	[11]
Colorimetric	Solution	AuNPs	20 min	900 ppm – 1500 ppm	500 ppm	Sodium nitrate, Sodium phosphate, $MgCl_2$, $ZnCl_2$, $SnCl_4$, Acetic acid, H_2SO_4, $FeCl_3$, HNO_3, HF	[6]
Colorimetric	Solution	GSH-AuNP aggregates	<1 s	3000 ppm – 10000 ppm	2875 ppm	H_2SO_4, HNO_3, H_3PO_4, HAc, H_3BO_3, oxalic acid, salicylic acid, NaCl, NaClO, HF, HBr, HI	This work

Table S3. Detection of HCl in real samples.

Sample	Method	Spiked (ppm)	Found (ppm)	Recovery (%)	RSD (%, n=3)
Tap water	Colorimetric	4000	4216	105.5	5.7
		8000	7936	92.2	0.9
		10000	9650	96.5	6.8
Yellow River water	Colorimetric	4000	4005	100.1	4.3
		8000	7285	91.0	3.2
		10000	10399	104.0	2.7
Lake water	Colorimetric	4000	4089	102.2	3.1
		8000	7707	96.3	1.6
		10000	10314	103.1	1.5
Industrial	Colorimetric	/	4997	/	1.3
wastewater		3000	7875	95.9	3.6
		5000	9532	90.7	3.9

Reference:

1. Y. Yu, Y. Hong, P. Gao and M. K. Nazeeruddin, *Analytical Chemistry*, 2016, **88**, 12316-12322.
2. L. Beqa, A. K. Singh, S. A. Khan, D. Senapati, S. R. Arumugam and P. C. Ray, *ACS Applied Materials & Interfaces*, 2011, **3**, 668-673.
3. L. Biao, S. Tan, Q. Meng, J. Gao, X. Zhang, Z. Liu and Y. Fu, *Journal*, 2018, **8**.
4. Z. Liu, Y. Zu, Y. Fu, R. Meng, S. Guo, Z. Xing and S. Tan, *Colloids and Surfaces B: Biointerfaces*, 2010, **76**, 311-316.
5. J. Zhang, W. Zheng and X. Jiang, *Small*, 2018, **14**, 1801680.
6. S. K. Tripathy, J. Y. Woo and C.-S. Han, *Analytical Chemistry*, 2011, **83**, 9206-9212.
7. A. Kovács and Z. Varga, *Coordination Chemistry Reviews*, 2006, **250**, 710-727.
8. M. Li, J. Tang, Y. Luo, J. Yang, J. Liu, J. Peng and Y. Fang, *Analytical Chemistry*, 2023, **95**, 2094-2101.
9. Z.-H. Zhu, Z. Ni, H.-H. Zou, G. Feng and B. Z. Tang, *Advanced Functional Materials*, 2021, **31**, 2106925.
10. C.-W. Zhao, J.-P. Ma, Q.-K. Liu, X.-R. Wang, Y. Liu, J. Yang, J.-S. Yang and Y.-B. Dong, *Chemical Communications*, 2016, **52**, 5238-5241.
11. C. Vervacke, C. C. Bof Bufon, D. J. Thurmer, P. F. Siles and O. G. Schmidt, *Analytical Chemistry*, 2012, **84**, 8399-8406.